Activin A Improves White Matter Injury in Neonatal Rats via Noggin/bmp4/id2 Signaling

Xiaojuan Su
West China Women\'s and Children\'s Hospital: Sichuan University West China Second University Hospital

Jun Tang
West China Women\'s and Children\'s Hospital: Sichuan University West China Second University Hospital

Lingyi Huang
Sichuan University West China College of Stomatology

Dongqiong Xiao
West China Women\'s and Children\'s Hospital: Sichuan University West China Second University Hospital

Xia Qiu
West China Women\'s and Children\'s Hospital: Sichuan University West China Second University Hospital

Junjie Ying
West China Women\'s and Children\'s Hospital: Sichuan University West China Second University Hospital

Shiping Li
West China Women\'s and Children\'s Hospital: Sichuan University West China Second University Hospital

Rina Pradhan
West China Women\'s and Children\'s Hospital: Sichuan University West China Second University Hospital

Qian Liu
West China Women\'s and Children\'s Hospital: Sichuan University West China Second University Hospital

Fengyan Zhao
West China Women\'s and Children\'s Hospital: Sichuan University West China Second University Hospital

yi Qu (quyi712002@163.com)
Sichuan University https://orcid.org/0000-0002-9993-8810

Dezhi Mu

West China Women\'s and Children\'s Hospital: Sichuan University West China Second University Hospital

Research

Keywords: Activin A, Noggin/BMP4/Id2 signalling, myelination, oligodendrocyte progenitor cells, white matter injury

Posted Date: June 8th, 2021

DOI: https://doi.org/10.21203/rs.3.rs-568992/v1

Abstract

Background

Activin A (Act A) has been revealed to enhance the differentiation of oligodendrocyte progenitor cells (OPCs) in vitro. Here we aim to elucidate its roles and mechanisms in a rat model of white matter injury (WMI).

Methods

Act A was injected into the lateral ventricle of a hypoxia-ischemia induced WMI rat model. Hematoxylin & eosin staining was used to detect pathological changes. Immunofluorescence staining was used to assess OPC proliferation, migration, apoptosis, and differentiation. Myelin sheath and axon formation were detected via immunofluorescence staining, Western blotting, and electron microscopy. Behavioral assessment of rats was performed with the Morris water maze test.

Results

Act A attenuated the pathological damages, enhanced the formation of myelin sheath and myelinated axons and improved the behavior of WMI rats by promoting OPC proliferation and differentiation. However, Act A showed no significant effects on OPC migration or apoptosis. Interestingly, we found that Act A could enhance Noggin expression, which in turn inhibited the expression of bone morphogenetic protein 4 (BMP4) and inhibitor of DNA binding 2 (Id2). Furthermore, upregulation of Id2 completely abolished the protective effects of Act A in WMI.

Conclusions

Act A improves WMI in neonatal rats via Noggin/BMP4/Id2 signalling.

Background

With the rapid development of perinatal medicine, the survival rate of premature infants has been greatly improved. However, 40–50% of the surviving premature infants show varying degrees of cognitive and behavioral disorders, and 5%–10% of preterm infants, especially the very low birth weight (<1 kg) preterm survivors, are diagnosed with white matter injury (WMI) [1]. WMI is a major form of neonatal brain injury induced by perinatal hypoxia-ischemia (HI), especially between 23 and 32 weeks of gestational age, corresponding to the peak of the myelination formation. WMI leads to long term functional impairments, including cognitive delay, cerebral palsy, and neurosensory impairments, and seriously affects the children's survival and quality of life, while imposing a serious burden on families and society. Unfortunately, specific therapies to promote the functional recovery from WMI are still unavailable [2].

The axons of the vertebrate central nervous system (CNS) are generally ensheathed by myelin, a tight spiral wrap of plasma membrane made by oligodendrocytes. Myelin-wrapped axons are the major

mediators of signal transduction in the CNS, and their formation is fundamental for brain development and function [3]. The myelin sheath is the major component of the white matter, which is formed by mature oligodendrocytes (OLs) differentiated from oligodendrocyte progenitor cells (OPCs) [4]. Mounting evidence suggests that OPCs are the key insulted cells when WMI occurs, resulting in a wave of acute immature OLs death and the inhibition of OPCs differentiation, finally hindering myelination and blocking the formation of ensheathed axon [5]. Therefore, enhancing OPC differentiation via endogenous or exogenous molecules might be a powerful strategy to promote myelination in WMI.

Activin A (Act A) is a widely expressed homodimer composed of two β_A chains. Sequence analysis showed that β subunit of Act A has the typical structural features of the transferring growth factor-β superfamily, and the mature human β_A chain of Act A has 100 % amino acid sequence identity in cattle, cats, mice, pigs, etc., indicating its highly conserved structure [6]. In the nervous system, Act A can be secreted by both neurons and glial cells, which exert neuroprotective effect. Previous studies have found that adding recombinant Act A protein to OPCs cultured in vitro promoted OPC proliferation and differentiation [7]. However, the role of Act A in neonatal WMI and the mechanisms involved are unknown.

In the present study, we established a WMI model in 5-day postnatal (P5) Sprague-Dawley (SD) rats, and examined whether exogenous Act A treatment contributes to the recovery of WMI. Besides, the potential mechanisms underlying the role of Act A in WMI were also explored.

Methods

Animals and WMI modeling

P5 SD rats (average weight 10–15 g) were purchased from Sichuan Dashuo Animal Science and Technology Co., Ltd (Chengdu, China). The rats were randomly divided into four groups: a Sham-operated group (Sham); a WMI model group (WMI); a group receiving Act A / phosphate-buffered saline (PBS) treatment after 24 h of WMI modeling (Act A/ PBS); and a group receiving Id2 overexpression lentiviral vector (Id2) and its corresponding vehicle(V), 6 h after Act A treatment (Id2/V).

The WMI model was established using the following procedure [8](Back, 2017): First, P5 neonatal rats were fixed on their backs after general anesthesia. The neck skin was then longitudinally incised for a length of about 1cm, and the right carotid artery was exposed and ligated after separation from glands and muscle tissue. After surgery, the rats were returned into an incubator for 30 min to recover. Then, they were placed in an 8%-oxygen and 92%-nitrogen cabin (8% O_2 and 92% N_2) with a gas flow rate of 3 L/min for 2 h to induce WMI. Rats were kept on a heating pad during surgical procedures to maintain the body temperature at 36–37 ^{o}C. The rats of the Sham group were only subjected to neck incision for dissociating the right carotid artery, without ligation or hypoxia. Following surgery, all neonatal rat pups were returned to their cages.

Drug treatment

To establish the Act A/PBS group, rats were injected with 5ul of Act A (12.5 mg/kg, 25 mg/kg, 50 mg/kg)/PBS after 24 h of WMI induction using a Hamilton syringe needle (Hamilton, USA) via the lateral ventricle (LV), located 2 mm posterior and 2 mm lateral (right) from the bregma with a 2 mm needle depth. 4 ul of Id2 overexpression lentiviral vector/vehicle was injected via the LV after 6 h of Act A treatment to establish the Id2/V group.

Hematoxylin & eosin staining

At P7, rats were sequentially perfused with 0.9% normal saline and 4% paraformaldehyde (100 mL each), after which the tissues were extracted and post-fixed in a 4% paraformaldehyde solution for 24–36 h at 4 ^{o}C. Then, the tissues were paraffin-embedded and serial sectioned in coronal position for 5mm, and three sections containing corpus callosum (CC) (0.26mm-1.80mm behind the anterior fontanelle according to the mapping of rat brain) were selected for analysis. Finally, the sectioned tissues were stained with hematoxylin & eosin (HE) and observed using a Leica inverted optical microscope (Leica, Germany). In each animal, four randomly selected fields were examined. Six animals per group were analyzed.

Immunofluorescence staining

Brains were taken at P7, P14, P21, P28, and P35 and post-fixed in 4% paraformaldehyde at 4^{o}C for at least 48 h, then embedded in 2–3% agarose. Coronal brain sections (thickness 40 μm) were cut using an oscillating tissue slicer (Leica, Germany). Three sections containing CC (0.26 mm-1.80 mm behind the anterior fontanelle according to the mapping of rat brain) were selected for analysis. The sections were first washed in PBS and incubated in 0.3% Triton X-100 at room temperature for half an hour, and then incubated for 1 h in fetal calf serum to inhibit non-specific binding. Second, the brain sections were incubated with the primary antibodies (rabbit anti-Id2 polyclonal antibody,1:500, novusbio; rabbit anti-BMP4 polyclonal antibody, 1:1000, abcam; rabbit anti-Olig2 polyclonal antibody, 1:500, Millipore; rabbit anti-Ki67 polyclonal antibody, 1:500, abcam; mouse anti-Vimentin monoclonal antibody, 1:200, abcam; rabbit anti-CC3 polyclonal antibody, 1:500, Cell signaling; rabbit anti-NG2 monoclonal antibody, 1:200, Proteintech; rabbit anti-O4 monoclonal antibody, 1:25, Millipore; mouse anti-APC antibody [CC-1], 1:200, abcam; mouse anti-MBP monoclonal antibody, 1:1000, arigo; rabbit anti-MAG monoclonal antibody, 1:100, CST; rabbit anti-PLP polyclonal antibody, 1:1000, abcam; mouse anti-Tau1 monoclonal antibody, 1:1000, Millipore; mouse anti-SMI31 monoclonal antibody, 1:1000, biolegend; mouse anti-SMI312 monoclonal antibody,1:1000, biolegend) at 4 ^{o}C overnight, then incubated for 2 h at room temperature with secondary antibodies which were Cy3-conjugated donkey anti-rabbit IgG, Cy3-conjugated donkey anti-mouse IgG, 488-conjugated donkey anti-rabbit IgG, 488-conjugated donkey anti-mouse IgG. The sections were mounted onto glass slides with Fluorescent Mounting Medium (Beyotime, China). Finally, fluorescence imaging was performed using a confocal laser scanning microscope (Olympus, Japan) and FV-ASW-3.1 software (Olympus). The mean fluorescence intensity was defined as the ratio between the sum of the integral optical density of the target protein and the area. Positive cells and mean fluorescence intensity counting were performed for each field with a 40X objective lens (field size, 0.24

mm^2), using the Image J software. In each animal, four randomly selected fields from the CC were examined. Six animals per group were analyzed.

Western blotting

The isolated CC was treated with a brain tissue protein extraction kit (Chengdu beibokit, BB-31227-1). Lysates were centrifuged at 14,000 rpm for 30 min at 4 °C. The protein concentration was determined through a BCA protein assay kit (Pierce) using bovine serum albumin (BSA) as the standard. Protein samples were separated on sodium dodecyl sulfate (SDS)-polyacrylamide gels. The protein was then transferred to polyvinylidene difluoride (PVDF) membranes, which were blocked in 5% non-fat dry milk in TBS containing 0.05% Tween 20 for 1 h at room temperature, with rotation. The membranes were then incubated overnight at 4 °C with the primary antibodies: rabbit anti-Act A polyclonal antibody (1:500, novusbio), mouse anti-MBP monoclonal antibody (1:500, arigo), rabbit anti-MAG monoclonal antibody (1:100, CST), rabbit anti-PLP polyclonal antibody (1:500, abcam), mouse anti-Tau1 monoclonal antibody (1:500, Millipore), mouse anti-SMI31 monoclonal antibody (1:500, biolegend), mouse anti-SMI312 monoclonal antibody (1:500, biolegend), mouse anti-Noggin monoclonal antibody (Abcam,1:200), rabbit anti-BMP4 polyclonal antibody (1:500, abcam), rabbit anti-Id2 polyclonal antibody (1:500, novusbio), and a mouse anti-actin polyclonal antibody (Santa Cruz Biotechnology, 1: 5000) was detected as the loading control. Following washes, the membranes were incubated with peroxidase conjugated goat anti-rabbit IgG or goat anti-mouse IgG (Santa Cruz Biotechnology, 1: 5000) in blocking solution for 1 h. The bound antibodies signals were developed by enhanced chemiluminescence (Pierce, Rockford, IL). The immunoreactivity of the signal bands was quantified using the Image J software. The relative expression level of the target protein was calculated as the target protein integrated density values (IDVs) relative to actin IDVs. All experiments were repeated at least three times to ensure the reproducibility of the results.

Electron microscopy

Rats were sequentially perfused with 0.9% normal saline and 4% paraformaldehyde (100 ml each) at P35. The rat brains were taken and sectioned to the size of approximately 1 mm^3 including the CC at 1.2 mm to 3.0 mm posterior to the bregma. The sectioned tissue was pre-fixed with a mixed solution of 3% glutaraldehyde. Then post-fixed in 1% osmium tetroxide, dehydrated in an acetone series, filtrated in Epox 812, and embedded. Next, the semi-thin sections were stained with methylene blue, the ultrathin sections were stained with uranyl acetate and lead citrate. Finally, the ultrathin sections were examined with a transmission electron microscope (EM) (H-600IV; Hitachi, Japan). Myelinated axons were counted for each field using the Image Pro Plus 6.0 software. In each animal, four randomly selected fields from the CC were examined. Six animals per group were analyzed.

Morris water maze

Behavioral testing using the Morris water maze (MWM) was performed from P29 to P35. The testing facilities includes a circular tank (1.5 m in diameter) and a location-constant platform (14 cm in diameter) placed 1.5 cm under the surface of the water. The water temperature was maintained at 25±1

^{o}C during testing. The test consists of two parts, namely place navigation training and space exploration, both of which are aimed to test spatial learning and memory ability.

The place navigation training was conducted during the first 6 days (P29–P34), For which the rats were trained to swim in the four alternating quadrants. From each quadrant, the rats swim in the water for 120 s. If the platform is successfully found during this period, the escape latency is recorded as the time at which the rats find the platform. If the rats fail to find the platform within 120 s, it is guided to it by a researcher and stays on the platform for 30 s, and the escape latency time being recorded as 120 s. The time at which the rat found the platform in each training session was recorded, and the average of the four quadrant latency periods was computed as a daily final score representing the ability to acquire the spatial information.

The platform was removed and the space navigation test was conducted at P35 to test the memory retention ability of the rats, 24 h after the last place navigation training. The rats were free to swim in the tank for 120 s from the third quadrant starting point. The trials were recorded using a video camera on the ceiling, and the platform crossing time was calculated and analyzed using the tracking system (Mengtai, China).

Quantification analysis and statistics

All images were acquired from the same CC area. All data were presented as mean ± standard deviation (SD). All graphs were produced using GraphPadPrism 8.0. A Student's t-test was used when comparing between two groups. Analysis of variance (ANOVA) was used when comparing more than two groups, followed by the Student’s t-test if homogeneity of variance was assumed or by Dunnett’s test if homogeneity of variance was not assumed. All statistical analyses were performed using SPSS 23.0. P-values *P <0.05, or **P < 0.01 were considered statistically significant.

Results

HI attenuated the expression of endogenous Act A in the rat brain

According to the developmental characteristics of rat brain, we set a time course for each assay, displayed as a schematic diagram in Figure 1A. We conducted Western blotting to detect the endogenous expression of Act A. It showed that Act A expression was reduced in the WMI group compared with the Sham group (Figure 1B), indicating that HI leads to evident reduction of Act A expression in neonatal rats.

Act A alleviated pathological damage of WMI rats

To detect the distribution of Act A after injected via the LV, we made Act A-EGFP protein and conducted immunofluorescence tracing. Fluorescence scanning showed that Act A-EGFP distributed in the cortex and white matter (including CC) from day 1 to day 28 after LV injection (Figure 1C). To select the optimal usage of Act A for WMI therapy, we used three dose concentrations (low, 12.5 mg/kg; medium, 25 mg/kg;

and high, 50 mg/kg) and three time points (12 h, 24 h and 48 h) for Act A administration after HI. We examined the pathological changes in the brain white matter and liver via hematoxylin & eosin (HE) staining, and detected rat weight at P14. HE staining for white matter showed that Act A improved necrosis and liquefaction after 24 h of HI (Figure 1D). The medium and the high doses of Act A gave better results than the low dose, while the difference between the medium and the high dose was not obvious (Figure 1D). However, hepatic HE staining at P21 and body weight analysis showed that the high dose rats underwent more liver damage, with lower body weight and poor state (Figure 1D). Therefore, the subsequent experiment was performed with the medium dose of Act A (25 mg/kg). To detect the overall expression level of Act A in the brain after exogenous Act A injection, we conducted western blotting at P6. It showed that Act A was abundantly expressed in the Act A group, as compared with the PBS group (Figure 1E). Collectively, these results suggest that Act A was successfully upregulated in WMI via exogenous Act A supplement.

Act A treatment promoted OPC proliferation and differentiation in the neonatal rat brain after HI

OPCs are the primarily insulted cells when WMI occurs. We next examined whether Act A affects OPC function in vivo. At P7, we investigated the proliferation, migration and apoptosis of OPCs via double immunostaining of Olig2 with Ki67, Vimentin, and CC3, respectively. It showed that the number of Ki67/Olig2 positive cells was significantly increased in the Act A treatment group compared with the PBS group (Figure 2A). However, the number of Vimentin/Olig2 (Figure 2B) and CC3/Olig2 positive cells (Figure 2C) was not different in the Act A group compared with the PBS group. Furthermore, we examined whether Act A contributes to the differentiation of OPCs to OLs. At P7 and P14, we quantified the number of OPCs in the white matter via double immunostaining of Olig2 with the OPCs specific marker NG2 among the experimental groups. It showed that the number of NG2/Olig2 positive cells and the mean NG2/Olig2 fluorescence intensity at both time points were significantly increased in the Act A group compared with the PBS group (Figure 3A). Then, at P14 and P21, we quantified the number of pre-oligodendrocytes (pre-OLs) in the white matter by double immunostaining Olig2 with the pre-OLs specific marker O4 among the experimental groups. As expected, the number of O4/Olig2 positive cells and the mean O4/Olig2 fluorescence intensity were also significantly increased at both time points in the Act A group compared with the PBS group (Figure 3B). Next, at P21 and P28, we performed double immunofluorescence staining of the mature OLs marker CC1 with Olig2 in the white matter. It showed that the number of CC1/Olig2 positive cells and the mean CC1/Olig2 fluorescence intensity were significantly increased in the Act A group compared with the PBS group (Figure 3C). Together, these results indicate that Act A promotes the proliferation and differentiation of OPCs, whereas it shows no significant effect on OPC migration and apoptosis.

Act A treatment promoted myelination and axon formation in the neonatal rat brain after HI

We then examined the myelination of the white matter by assessing the expression of MBP, PLP, and MAG through immunostaining and western blotting. At P28, the expression of MBP, PLP, and MAG was significantly enhanced in the Act A group compared with the PBS group (Figure 4A). Consistently, at P35,

the expression of the axon markers Tau1, SMI31, and SMI312, was significantly increased in the Act A group compared with the PBS group (Figure 4B). At P35, EM also showed more myelinated axons in the CC of brains in the Act A group compared with the PBS group (Figure 4C). Collectively, these results indicate that exogenous Act A supplement in neonatal WMI contributed to the long-term recovery of myelination and axon formation.

Act A treatment enhanced the behavioral performance of WMI rats.

The MWM test was conducted to compare the behavioral abilities among the experimental groups from P29 to P35, by calculating the average escape latency and platform crossing times during swimming. It showed that the average escape latency was significantly decreased from P31 in the Act A group compared with the PBS group (Figure 5A), and the frequency of platform crossing was significantly increased at P35 in the Act A group compared with the PBS group (Figure 5B). These results suggest that the exogenous Act A supplement contributes to the long-term behavioral improvements in terms of learning and memory.

Act A treatment enhanced the expression of Noggin, while inhibited BMP4/Id2 expression.

We then examined the possible down-stream effectors of Act A. At P21, we performed immunofluorescence staining to assess the expression of bone morphogenetic protein 4(BMP4) and inhibitor of DNA binding 2(Id2) among Sham, PBS and Act A groups. We found that they were significantly increased in the PBS group compared with the Sham group (Figure 6A-B), while significantly decreased after Act A treatment (Figure 6A-B). Consistently, Western blotting was conducted to detect Noggin/BMP4/Id2 expression. It showed that Noggin expression was significantly enhanced in the Act A group compared with the PBS group, whereas both BMP4/Id2 proteins showed a significant downregulation in the Act A group compared with the PBS group (Figure 6C). Collectively, these findings suggest that Id2 might be the down-stream effector of Act A, which might be activated through Noggin/BMP4 signaling.

Id2 is the crucial downstream effector of Act A in WMI

To further verify that Id2 is the key downstream effector of Act A in WMI, we overexpressed it in the Act A group with an Id2 overexpression lentiviral vector ($1x10^9$TU/ml), a corresponding vehicle-only (V) group was set up as the control. Fluorescence scanning showed that Id2-EGFP (green fluorescence) distributed in the cortex and white matter (including CC) for up to 4 weeks. On the first day after injection, Id2-EGFP has already appeared in the CC (white arrow) and cortex (red arrow). From the 7th day to the 21st day after injection, the fluorescence intensity of Id2-EGFP in the CC and cortex is significantly increased, whereas on the 28th day after injection, the fluorescence intensity of Id2-EGFP in the CC and cortex is reduced significantly (Figure 7A). At P21, we performed immunofluorescence staining and Western blotting to detect Id2 expression in the V and Id2 groups. It showed that Id2 was significantly increased in the Id2 group compared with the V group (Figure 7B).

The effects of Id2 overexpression were further examined. HE staining at P7 showed more white matter necrosis in the Id2 group compared with the V group (Figure 7C). Id2 overexpression did not affect the proliferation of OPCs, as indicated by the immunofluorescence staining and statistical analysis of Ki67/Olig2 positive cells, which were not significantly different between the V and Id2 groups (Figure 8A). Regarding OPC differentiation, using different time points (from P7 to P28) corresponding to specific differentiation stages, we found that the number of positive cells and the mean fluorescence intensity for NG2/Olig2, O4/Olig2 and CC1/Olig2 (Figure 8B) were significantly decreased in the Id2 group compared with the V group. Consistently, we found that overexpression of Id2 attenuated the expression of MBP, PLP, and MAG at P28 (Figure 9A), as well as that of Tau1, SMI31, and SMI312 at P35 (Figure 9B) after Act A treatment, as indicated by immunofluorescence staining and western blotting. Similarly, at P35, EM showed less myelinated axons in the Id2 group compared with the V group (Figure 9C). The MWM test showed that the average escape latency was significantly increased from P31 in the Id2 group compared with the V group (Figure 10A), and the frequency of platform crossing significantly decreased at P35 in the Id2 group compared with the V group (Figure 10B). The performance of the Id2 group was similar to that of the PBS group, suggesting that Id2 overexpression triggers the restoration of behavioral dysfunction. Collectively, these results indicated that Id2 overexpression reversed the effect of Act A in WMI, suggesting that Id2 is the crucial downstream effector of Act A in WMI.

Discussion

As OPCs are the major insulted cells in WMI, protecting OPCs has become the key strategy for WMI recovery [9]. Recent reports of the involvement of Act A in the regulation of OPC maturation in vitro led us to examine its role in WMI in vivo [3]. In an adult rat model of focal cerebral ischemia that simulates a stroke, it was found that the expression of Act A protein around the infarction was higher than that of normal rats [10]. However, in this study, we found that the expression of endogenous Act A was significantly reduced after WMI in newborn rats. We suspect that this discrepancy may be due to the differences in the age of rats and the models constructed. We try to replenish a certain dose of Act A externally to compensate for the decrease in Act A caused by WMI. Considering the obstacles of the blood brain barrier, we tried to inject Act A via the lateral ventricle in the rat model of WMI. The Act A-EGFP tracing experiment showed that Act A-EGFP protein was distributed in the cerebral cortex and white matter (including the CC) from day 1 to day 28 after injection, indicating that after lateral ventricle injection, Act A can enter and exist in the brain for up to 4 weeks, ensuring its efficacy after just one injection. To explore the therapeutic time window of Act A molecules, we set up injections before and after molding, single injection and continuous multiple injections in our preliminary study, and found that the effect of injection before molding is better than injection after molding, but the effect of multiple injections and single injection is not obvious. Considering that the injection before the model is difficult to simulate the actual clinical treatment, we decided to adopt the injection program after the model. Next, three different concentrations of Act A were analyzed to determine the optimal dosage. We found that the medium dose of Act A led to WMI recovery without obvious side effects. Although lateral ventricle injection is a powerful medication method, it is a traumatic operation, which will limit its clinical usage.

Recently, some non-traumatic methods bringing drugs into the brain overcoming the blockage of the blood brain barrier have emerged, mostly based on material-based deliveries. For example, in 2012, Wang et al. effectively delivered a glial cell-derived neurotrophic factor to the brain of rats via conjugated-biotinylated lipid-coated microbubbles [11]. Our future work will explore more feasible pathways to deliver Act A into the brain.

According to the brain developmental characteristics of rats, the formation of myelin sheath wrapped axons undergoes several successive stages, starting from OPC differentiation [8]. OPC differentiation occurs mainly in the first week after birth and continues into the next week. The main process during the late second week after birth is the formation of pre-OLs, while the third week after birth is used for the formation of OLs. The myelin sheath, which wraps the axons to provide the basis for the transmission of neural signals, is mostly formed later [12]. In the present study, we set different time points for the detection of the progressive differentiation and maturation of OLs: P7 and P14 for the detection of OPCs, P14 and P21 for the detection of pre-OLs, P21 and P28 for the detection of OLs, P28 for the detection of myelin formation, and P35 for the detection of myelin-wrapped axons. This experimental design allowed us obtaining an overall perspective of how Act A affects the progression of WMI.

Previous studies revealed that Act A exerts its neuroprotection roles mainly through Smad-dependent pathways. Recently, it was indicated that Act A can exert its function through Smad-independent pathways such as nuclear factor-κB, extracellular signal-regulated kinase (ERK1/2), ubiquitin-proteolytic, mitogen-activated protein kinase (MAPK), and AKT pathways [13]. Our study revealed that the repairing effect of exogenous Act A on WMI of newborn rats is mainly achieved by promoting the differentiation and maturation of OLs. Previous studies have reported that the Id2 participates in different stages of OLs differentiation and is a key molecule that regulates the differentiation and maturation of OLs [14]. Id2 can inhibit the expression of myelin formation genes and keep OPCs in an undifferentiated state, thereby inhibiting the differentiation of OPCs and the production of mature OLs [15]. Based on these existing reports, we overexpressed Id2 in WMI rat model and confirmed that it was the crucial downstream effector of Act A. Then we want to clarify how Act A regulates Id2. Numerous studies have found that Act A can regulate cell differentiation by interacting with BMP4[16-19], while BMP4 can regulate the differentiation and maturation of OLs by regulating its downstream target molecule Id2. The BMP4/Id2 signal will hinder the differentiation of OPCs into OLs [20]. At the same time, Noggin is a key upstream molecule regulated by BMP4. Increased Noggin expression can inhibit BMP4 expression, while Act A can enhance Noggin expression [21, 22]. Therefore, we speculate that the regulatory effect of Act A on Id2 may be achieved through the Noggin/BMP4 pathway. Therefore, we detected the expression of Noggin/BMP4/Id2 after WMI or Act A treatment. It showed that the expression of Noggin was inhibited after WMI, while the expression of BMP4 and Id2 was increased. After Act A treatment, the expression of Noggin was significantly upregulated, while the expression of BMP4 and Id2 was significantly downregulated. Besides, Overexpression of Id2 blocked the repairing effect of Act A on WMI. Collectively, these results suggest that Act A might regulate Id2 through Noggin/BMP4 signaling. We speculate that Act A enters the intercellular space through diffusion after it is injected into the lateral ventricle, and binds to Act A receptors on the surface of OPCs, then activates the expression of Noggin, inhibits the expression

of BMP4 and Id2, thereby relieves the negative regulatory factors modulating OPC differentiation, then promoted the formation of myelin sheath, reduced the pathological damage of brain white matter, and finally repaired the neurobehavioral ability of rats. However, since the effects of blocking or overexpression of Noggin and BMP4 have not been tested, it is only a possible speculation that Act A regulating Id2 through the Noggin/BMP4 signaling. More evidence is needed to clarify its causality.

Conclusions

In summary, our study indicated that exogenous Act A treatment could protect WMI via Noggin/BMP4/Id2 signaling. Besides, our study also found that OPC proliferation was not significantly altered after Id2 overexpression, suggesting the presence of another mechanism by which Act A regulates OPC proliferation. Although Act A has been used as a diagnostic and prognostic biomarker for some brain diseases [23], it has not been used to treat brain damage in clinical practice. Our findings demonstrated for the first time that exogenous Act A treatment could alleviate WMI in the developing brain, providing a potential agent to treat neonatal WMI in the future. Besides, its roles in other types of white matter damage, such as multiple sclerosis and hereditary multi-infarct dementia, are worthy to be explored.

Abbreviations

Act A: activin A; OPCs : oligodendrocyte progenitor cells; WMI : white matter injury; HI: hypoxia-ischemia; HE: hematoxylin & eosin; MWM: Morris water maze; BMP4: bone morphogenetic protein 4; Id2: inhibitor of DNA binding 2; CNS: central nervous system; pre-OLs: pre-oligodendrocytes; OLs: oligodendrocytes; SD: sprague-dawley; P: Postnatal; PBS: phosphate-buffered saline; EM: electron microscopy; MAPK: mitogen-activated protein kinase; BSA: bovine serum albumin; SDS: sodium dodecyl sulfate; PVDF: polyvinylidene difluoride; CC: corpus callosum

Declarations

Ethics approval and consent to participate

This study was approved by the Research Animal Care Committee of Sichuan University, China. All procedures on animals were performed in accordance with the National Institute of Health Guide for the Care and Use of Laboratory Animals (NIH Publications No.8023).

Consent for publication

Not applicable

Availability of data and materials

All data generated or analyzed during this study are included in this published article.

Competing interests

The authors declare that they have no competing interests

Funding

This work was supported by the National Key Research Project (2017YFA0104200), National Natural Science Foundation of China (81630038, 81771634, 81842011, 81971433, 81971428), National Undergraduate Training Program for Innovation and Entrepreneurship (C2019104355, Sichuan University), and National Key Project of Neonatal Children (1311200003303).

Author contributions

XS, JT and YQ contributed to the conception and design of the research and the drafting of this article. XS and LH participated in the animal model establishment and immunostaining assay. JY, SL and R Pradhan participated in the molecular biological experiments. XS, DX, XQ, QL and FZ participated in the Morris water maze test. YQ and DM contributed to financial support for the studies.

Acknowledgments

We would like to thank Editage [www.editage.cn] for English language editing.

References

1. Alexandrou G, Martensson G, Skiold B, Blennow M, Aden U, Vollmer B: White matter microstructure is influenced by extremely preterm birth and neonatal respiratory factors. Acta paediatrica 2014, 103(1):48-56.
2. Gano D: White Matter Injury in Premature Newborns. Neonatal network : NN 2016, 35(2):73-77.
3. Snaidero N, Mobius W, Czopka T, Hekking LH, Mathisen C, Verkleij D, Goebbels S, Edgar J, Merkler D, Lyons DA et al: Myelin membrane wrapping of CNS axons by PI(3,4,5)P3-dependent polarized growth at the inner tongue. Cell 2014, 156(1-2):277-290.
4. Suzuki N, Sekimoto K, Hayashi C, Mabuchi Y, Nakamura T, Akazawa C: Differentiation of Oligodendrocyte Precursor Cells from Sox10-Venus Mice to Oligodendrocytes and Astrocytes. Sci Rep 2017, 7(1):14133.
5. Liu XB, Shen Y, Plane JM, Deng W: Vulnerability of premyelinating oligodendrocytes to white-matter damage in neonatal brain injury. Neuroscience bulletin 2013, 29(2):229-238.
6. Wang X, Fischer G, Hyvonen M: Structure and activation of pro-activin A. Nature communications 2016, 7:12052.
7. Goebbels S, Wieser GL, Pieper A, Spitzer S, Weege B, Yan K, Edgar JM, Yagensky O, Wichert SP, Agarwal A et al: A neuronal PI(3,4,5)P3-dependent program of oligodendrocyte precursor recruitment and myelination. Nature neuroscience 2017, 20(1):10-15.
8. Back SA: White matter injury in the preterm infant: pathology and mechanisms. Acta neuropathologica 2017, 134(3):331-349.

9. Wang F, Yang YJ, Yang N, Chen XJ, Huang NX, Zhang J, Wu Y, Liu Z, Gao X, Li T et al: Enhancing Oligodendrocyte Myelination Rescues Synaptic Loss and Improves Functional Recovery after Chronic Hypoxia. Neuron 2018, 99(4):689-701 e685.
10. Nishio S, Yunoki M, Chen ZF, Anzivino MJ, Lee KS: Ischemic tolerance in the rat neocortex following hypothermic preconditioning. Journal of neurosurgery 2000, 93(5):845-851.
11. Wang F, Shi Y, Lu L, Liu L, Cai Y, Zheng H, Liu X, Yan F, Zou C, Sun C et al: Targeted delivery of GDNF through the blood-brain barrier by MRI-guided focused ultrasound. PloS one 2012, 7(12):e52925.
12. Simons M, Nave KA: Oligodendrocytes: Myelination and Axonal Support. Cold Spring Harbor perspectives in biology 2015, 8(1):a020479.
13. Derynck R, Zhang YE: Smad-dependent and Smad-independent pathways in TGF-beta family signalling. Nature 2003, 425(6958):577-584.
14. Chen XS, Zhang YH, Cai QY, Yao ZX: ID2: A negative transcription factor regulating oligodendroglia differentiation. Journal of neuroscience research 2012, 90(5):925-932.
15. Samanta J, Kessler JA: Interactions between ID and OLIG proteins mediate the inhibitory effects of BMP4 on oligodendroglial differentiation. Development 2004, 131(17):4131-4142.
16. Lepletier A, Hun ML, Hammett MV, Wong K, Naeem H, Hedger M, Loveland K, Chidgey AP: Interplay between Follistatin, Activin A, and BMP4 Signaling Regulates Postnatal Thymic Epithelial Progenitor Cell Differentiation during Aging. Cell reports 2019, 27(13):3887-3901 e3884.
17. Yang S, Yuan Q, Niu M, Hou J, Zhu Z, Sun M, Li Z, He Z: BMP4 promotes mouse iPS cell differentiation to male germ cells via Smad1/5, Gata4, Id1 and Id2. Reproduction 2017, 153(2):211-220.
18. Olsen OE, Wader KF, Hella H, Mylin AK, Turesson I, Nesthus I, Waage A, Sundan A, Holien T: Activin A inhibits BMP-signaling by binding ACVR2A and ACVR2B. Cell communication and signaling : CCS 2015, 13:27.
19. Kim MS, Horst A, Blinka S, Stamm K, Mahnke D, Schuman J, Gundry R, Tomita-Mitchell A, Lough J: Activin-A and Bmp4 levels modulate cell type specification during CHIR-induced cardiomyogenesis. PloS one 2015, 10(2):e0118670.
20. Miyazono K, Miyazawa K: Id: a target of BMP signaling. Science's STKE : signal transduction knowledge environment 2002, 2002(151):pe40.
21. Koyano S, Fukui A, Uchida S, Yamada K, Asashima M, Sakuragawa N: Synthesis and release of activin and noggin by cultured human amniotic epithelial cells. Development, growth & differentiation 2002, 44(2):103-112.
22. Wijgerde M, Karp S, McMahon J, McMahon AP: Noggin antagonism of BMP4 signaling controls development of the axial skeleton in the mouse. Developmental biology 2005, 286(1):149-157.
23. Bergestuen DS, Edvardsen T, Aakhus S, Ueland T, Oie E, Vatn M, Aukrust P, Thiis-Evensen E: Activin A in carcinoid heart disease: a possible role in diagnosis and pathogenesis. Neuroendocrinology 2010, 92(3):168-177.

Figures

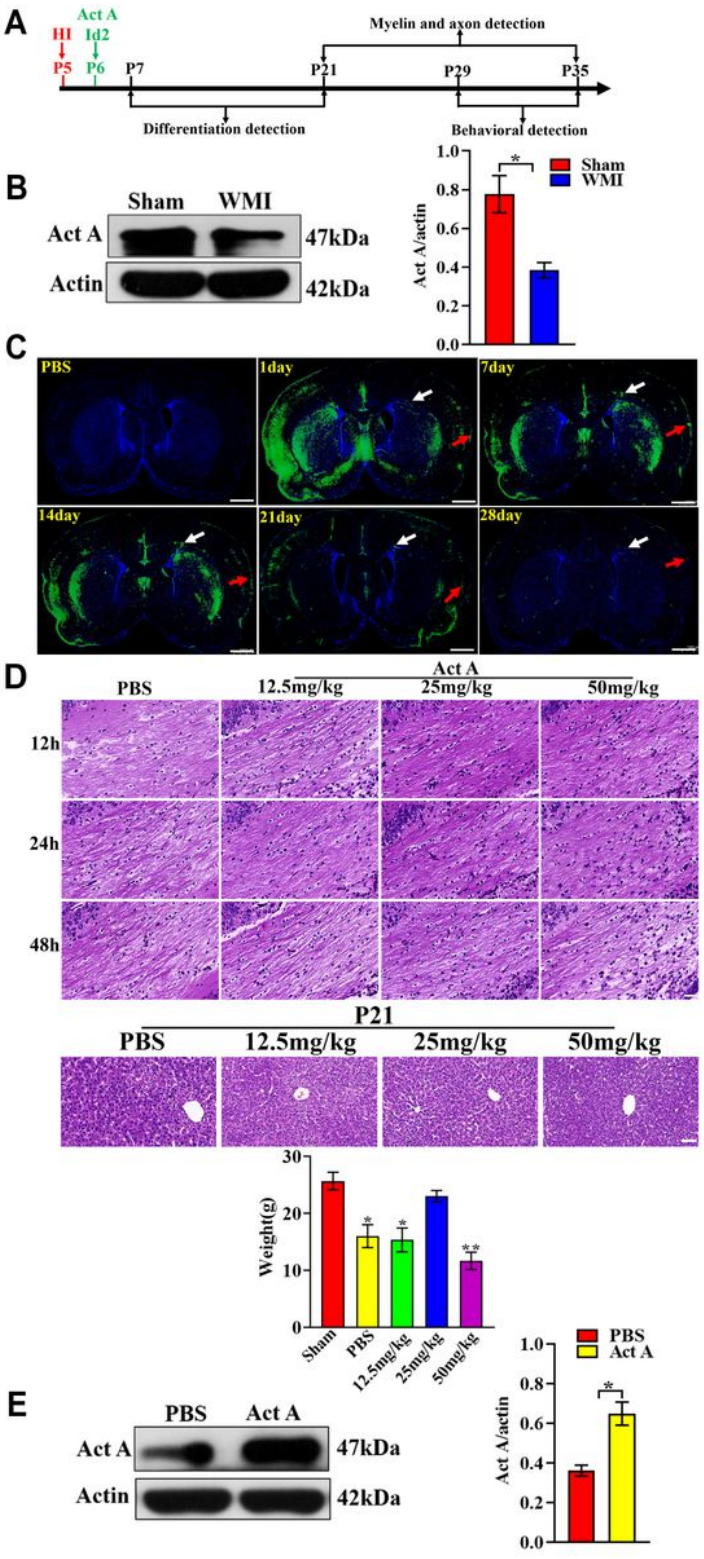

Figure 1

Act A treatment attenuated the pathological damages in WMI (A) Schematic diagram displaying the design of the animal experiment (B) Expression of endogenous Act A was decreased after WMI in neonatal rats Detection of Act A expression via Western blotting in the Sham and WMI groups. The

relative expression level of the target proteins was calculated as the integrated density value normalized to β-actin. (C) Immunofluorescence detection for Act A-EGFP after injected via the lateral ventricle Arrows indicate the Act A-EGFP (green fluorescence) positive area, Scale bar, 1000μm. (D) HE staining and weight statistics to select the optimal dose of Act A HE staining to evaluate the histopathologic damages of the CC area and the liver in PBS and Act A groups. Scale bar, 20 μm. Weight statistics of P14 in each group. P, postnatal day; CC, corpus callosum; PBS/Act A, group with PBS/Act A injected after WMI. (E) Detection of Act A expression after Act A treatment by Western blotting The expression of Act A was upregulated after Act A treatment.

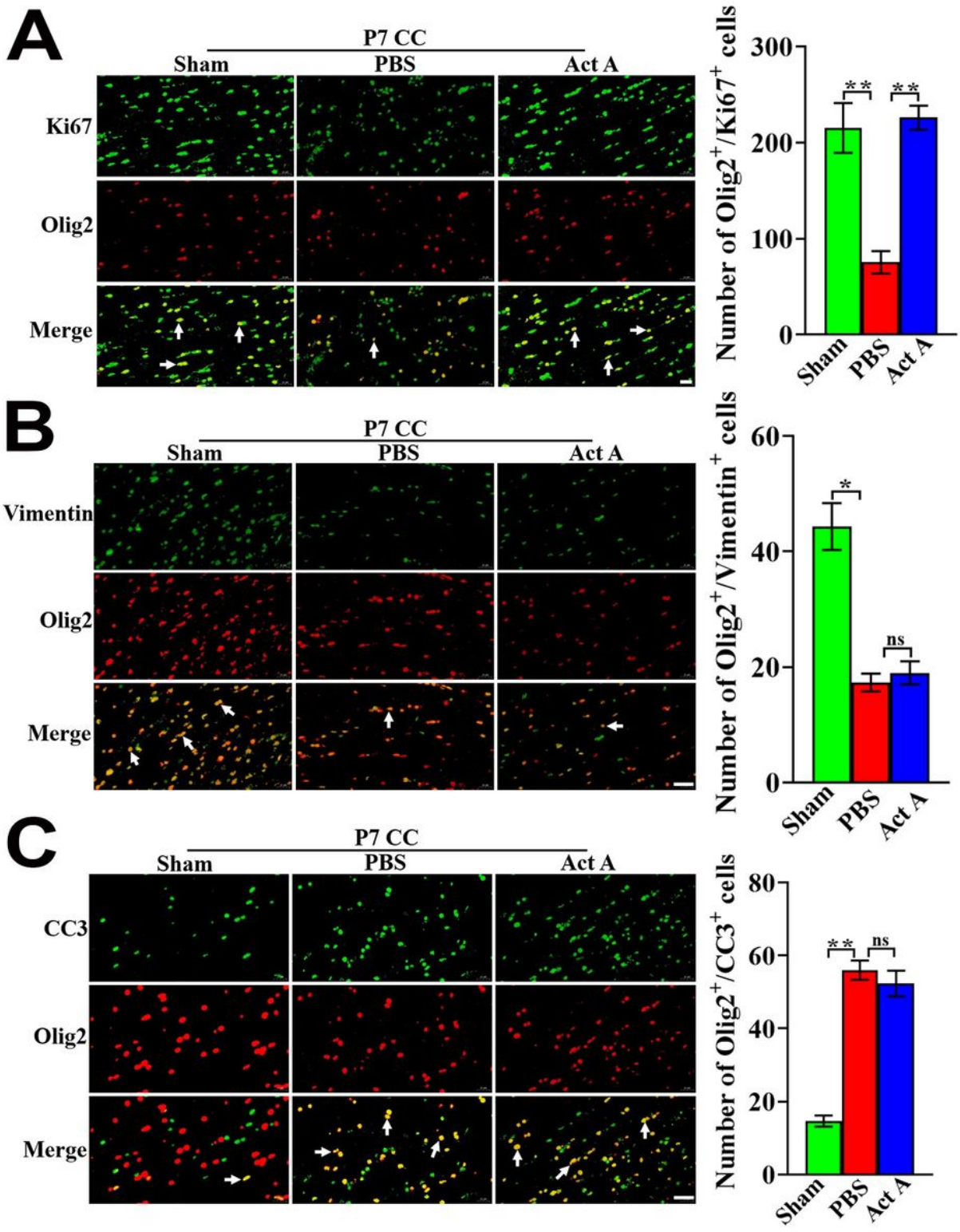

Figure 2

Act A treatment promoted OPC proliferation but did not affect OPC migration or apoptosis in the neonatal rat brain after WMI (A) Act A treatment promoted OPC proliferation Representative immunofluorescence staining images and quantification of Ki67 expression (green) in the CC via double staining with Olig2 (red). Arrows indicate the Ki67/Olig2 (yellow) positive cells. The positive cells counting was performed per field with a 40X objective lens (field size, 0.24 mm2), using the Image J software. It showed that the

number of Ki67/Olig2 positive cells was significantly increased in the Act A treatment group compared with the PBS group. Ki67, proliferation marker; Olig2, oligodendrocyte transcription factor. Scale bar, 20 μm. (B) Act A treatment did not affect the migration of OPC Representative immunofluorescence staining images and quantification of Vimentin (green) expression via double staining with Olig2 (red). Arrows indicate the Vimentin/Olig2 (yellow) positive cells. It showed that the number of Vimentin/Olig2 positive cells was not different in the Act A group compared with the PBS group. Vimentin, a migration marker. Scale bar, 20 μm. (C) Act A treatment did not affect the apoptosis of OPC Representative immunofluorescence staining images and quantification of CC3 expression (green) via double staining with Olig2(red). Arrows indicate the CC3/Olig2(yellow) positive cells. It showed that the number of CC3/Olig2 positive cells was not different in the Act A group compared with the PBS group. CC3, cleaved caspase 3, an apoptosis marker. Scale bar, 20 μm.

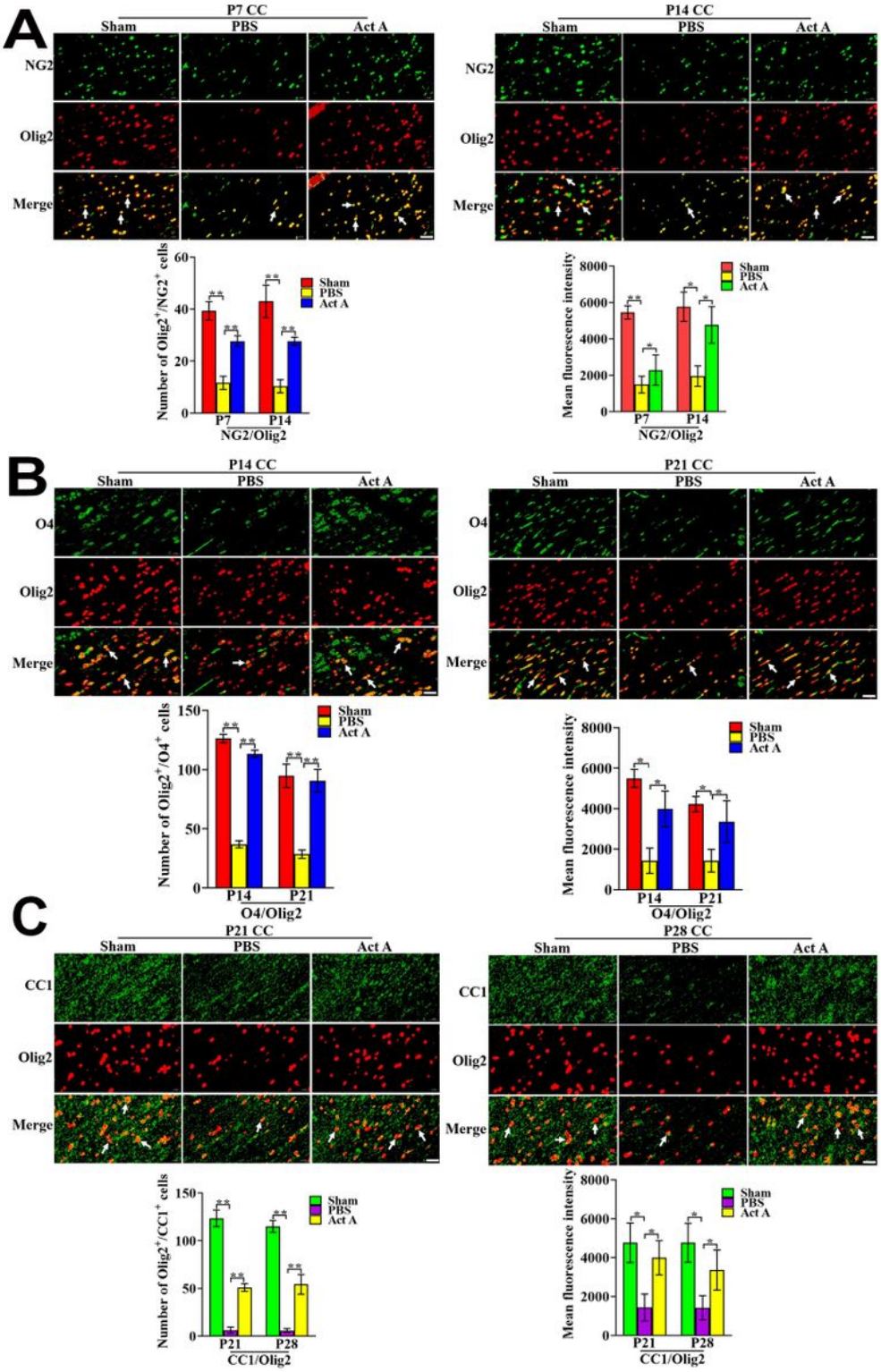

Figure 3

Act A treatment promoted OPC differentiation in the neonatal rat brain after WMI (A) Representative immunofluorescence staining images and quantification of NG2 (green) expression via double staining with Olig2 (red) at P7 and P14. Arrows indicate the NG2/Olig2 (yellow) positive cells. The number of NG2/Olig2 positive cells and the mean NG2/Olig2 fluorescence intensity were quantified. The mean fluorescence intensity was defined as the ratio of the sum of the integral optical density of the target

protein and the area. It showed that the number of NG2/Olig2 positive cells and the mean NG2/Olig2 fluorescence intensity at both time points were significantly increased in the Act A group compared with the PBS group. NG2, an OPCs marker. Scale bar, 20 μm. (B) Representative immunofluorescence staining images and quantification of O4(green) expression via double staining with Olig2(red) at P14 and P21. Arrows indicate the O4/Olig2 (yellow) positive cells. The number of O4/Olig2 positive cells and the mean O4/Olig2 fluorescence intensity were quantified. It showed that the number of O4/Olig2 positive cells and the mean O4/Olig2 fluorescence intensity were significantly increased at both time points in the Act A group compared with the PBS group. O4, a marker of pre-OLs. Scale bar, 20 μm. (C) Representative immunofluorescence staining images and quantification of CC1 (green) expression via double staining with Olig2 (red) at P21 and P28. Arrows indicate the CC1/Olig2(yellow) positive cells. The number of CC1/Olig2 positive cells and the mean CC1/Olig2 fluorescence intensity were quantified. It showed that the number of CC1/Olig2 positive cells and the mean CC1/Olig2 fluorescence intensity were significantly increased in the Act A group compared with the PBS group. CC1, Anti-APC (Activated protein C), a marker of mature oligodendrocytes. Scale bar, 20 μm.

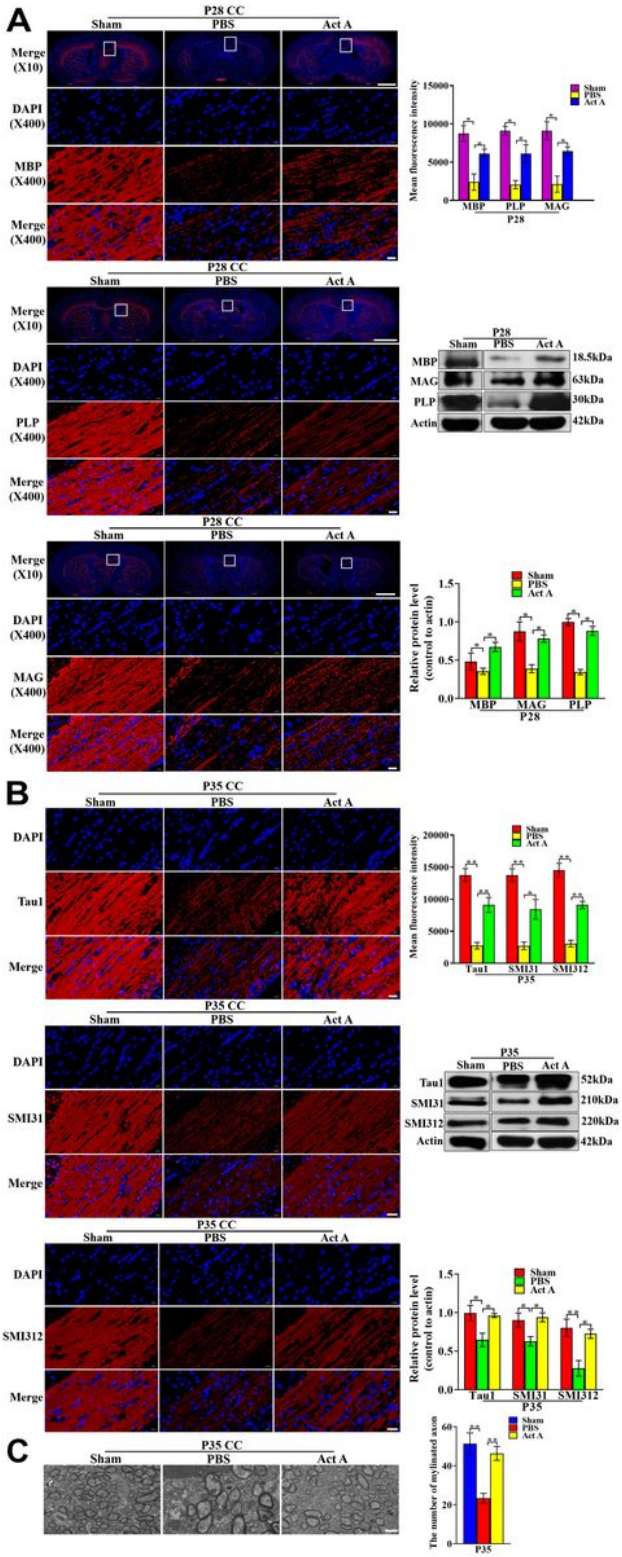

Figure 4

Act A treatment promoted myelination and axon formation in the neonatal rat brain after WMI (A) Act A treatment promoted myelination in WMI Representative immunofluorescence staining images and quantification of the expression of the myelin sheath markers MBP, PLP and MAG (red) at P28. Cell nuclei were labeled with DAPI (blue). The mean fluorescence intensity of MBP, PLP, and MAG was quantified. Western blotting and corresponding quantification were conducted to measure the expression of MBP,

PLP, and MAG at P28. It showed that the expression of MBP, PLP, and MAG was significantly enhanced in the Act A group compared with the PBS group. Scale bar, 1000 μm, 20 μm. (B) Act A treatment enhanced axon formation in WMI Representative immunofluorescence staining images and quantification of axons markers Tau1, SMI31, and SMI312 (red) at P35. The mean fluorescence intensity of Tau1, SMI31, and SMI312 was quantified. Western blotting and corresponding quantification were performed to measure the expression of Tau1, SMI31, and SMI312 at P35. It showed that the expression of Tau1, SMI31, and SMI312 was significantly increased in the Act A group compared with the PBS group. Scale bar, 1000 μm, 20 μm. (C) Act A treatment enhanced the formation of myelinated axons in WMI Representative EM images in the CC at P35. The number of myelinated axons was counted per field using the Image Pro Plus 6.0 software. It showed that the Act A group with more myelinated axons compared with the PBS group. Scale bar, 2 μm.

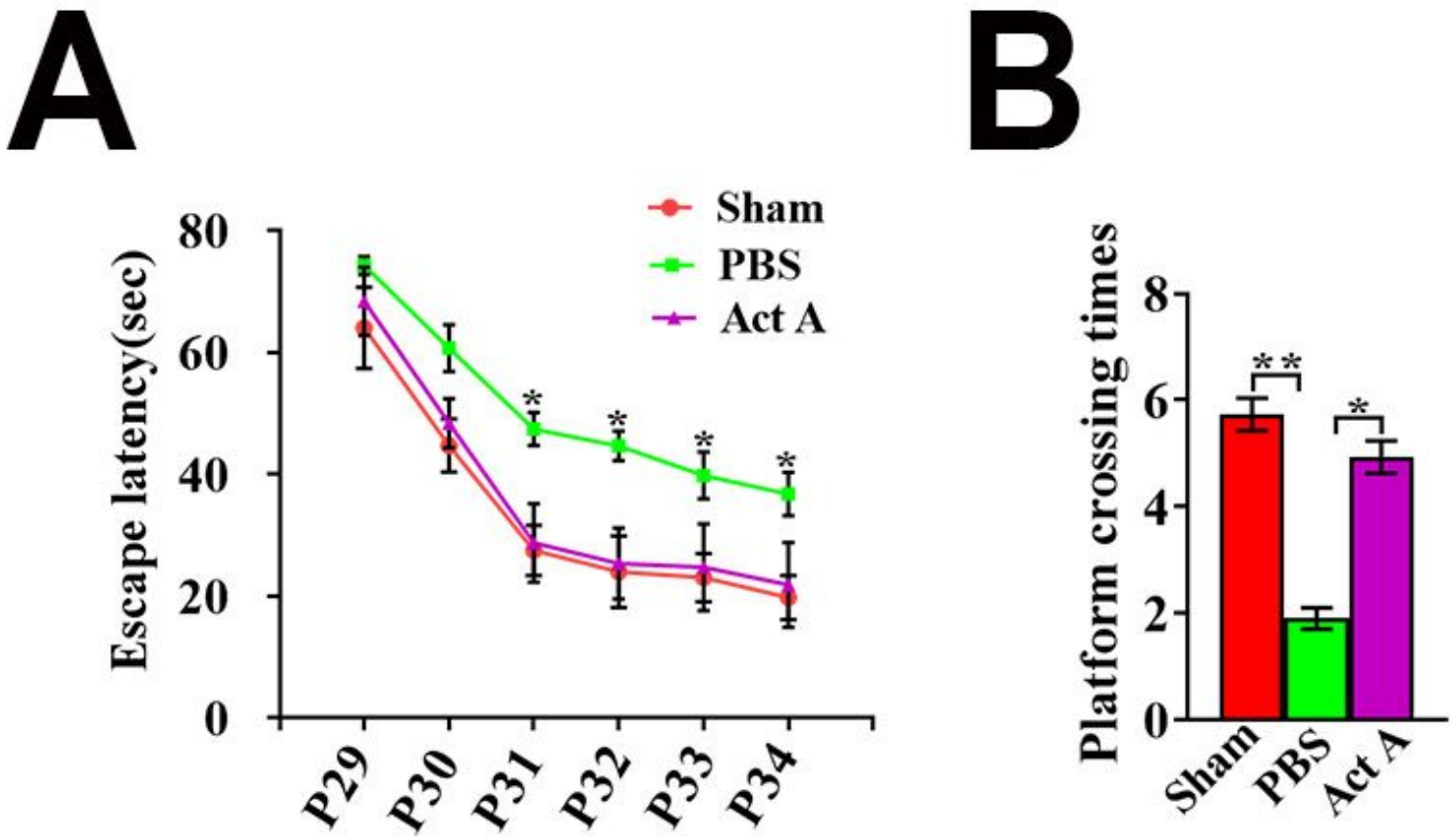

Figure 5

Act A treatment enhanced the behavioral performance of WMI rats (A) Daily average escape latency of SD rats during the training period The place navigation test was conducted and the escape latency was calculated to assess the acquisition of spatial information of rats. It showed that the average escape latency was greatly decreased in the Act A group compared with the PBS group. (B) The average platform crossing times of SD rats during the test period The space navigation test was conducted and the platform crossing times were calculated to evaluate the memory retention ability of rats. The frequency of platform crossing was significantly increased in the Act A group compared with the PBS group.

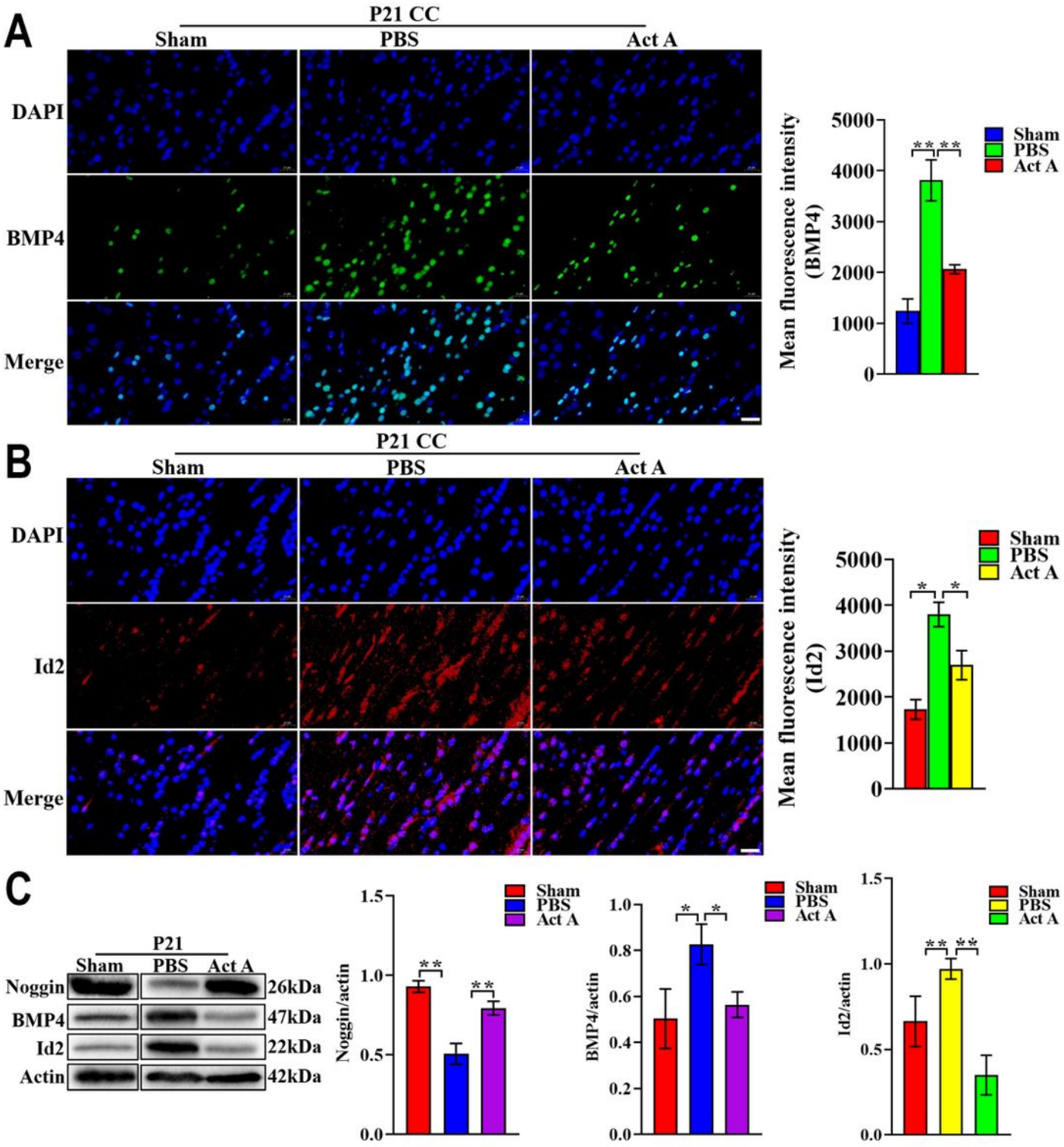

Figure 6

Act A treatment enhanced Noggin expression, while inhibited the expression of BMP4 and Id2 in WMI rats (A) Detection of BMP4 expression via immunofluorescence staining Representative immunofluorescence staining of BMP4 (green) expression at P21. Quantitative analysis of the mean fluorescence intensity of BMP4 was performed. It showed that the expression of BMP4 was significantly decreased in the Act A group compared with the PBS group. Scale bar, 20 μm. (B) Detection of Id2 expression by

immunofluorescence staining Representative immunofluorescence staining of Id2 (red) expression at P21. Quantitative analysis of the mean fluorescence intensity of Id2 was performed. It showed that the expression of Id2 was significantly decreased after Act A treatment. Scale bar, 20 μm. (C) Detection of Noggin/BMP4/Id2 expression by Western blotting Western blotting was performed to quantify the expression of Noggin/BMP4/Id2. It showed that the expression of Noggin was significantly upregulated in the Act A group compared with the PBS group, while BMP4/Id2 was significantly downregulated.

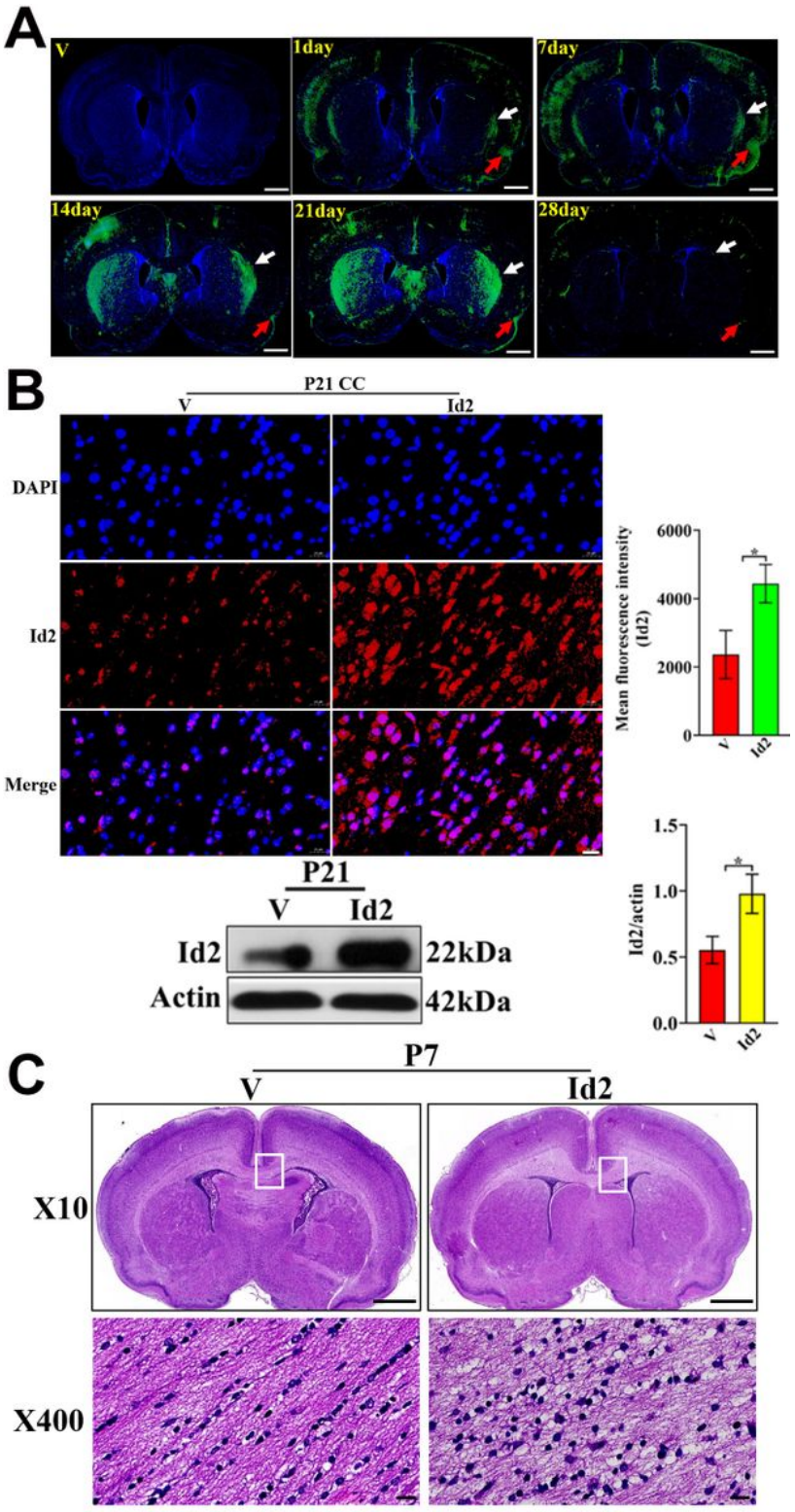

Figure 7

Overexpression of Id2 abolished the pathological improvement of Act A in WMI (A) Immunofluorescence staining for Id2-EGFP expression Arrows indicate the Id2-EGFP (green fluorescence) positive expression. Scale bar,1000 μm. (B) Detection of Id2 expression Representative immunofluorescence staining images of Id2(red) expression at P21. Quantitative analysis of the mean Id2 fluorescence intensity was performed. Western blotting and corresponding quantification were also conducted to compare the expression of Id2. It showed that Id2 expression was significantly increased in the Id2 group compared with the V group. V/Id2, group in which vehicle/Id2 overexpression lentiviral vector was injected after 6h of Act A treatment. Scale bar, 20 μm. (C) HE staining to evaluate the histopathologic damages in the V and Id2 group. HE staining showed more white matter necrosis in the Id2 group compared with the V group. Scale bar, 1000 μm, 20 μm.

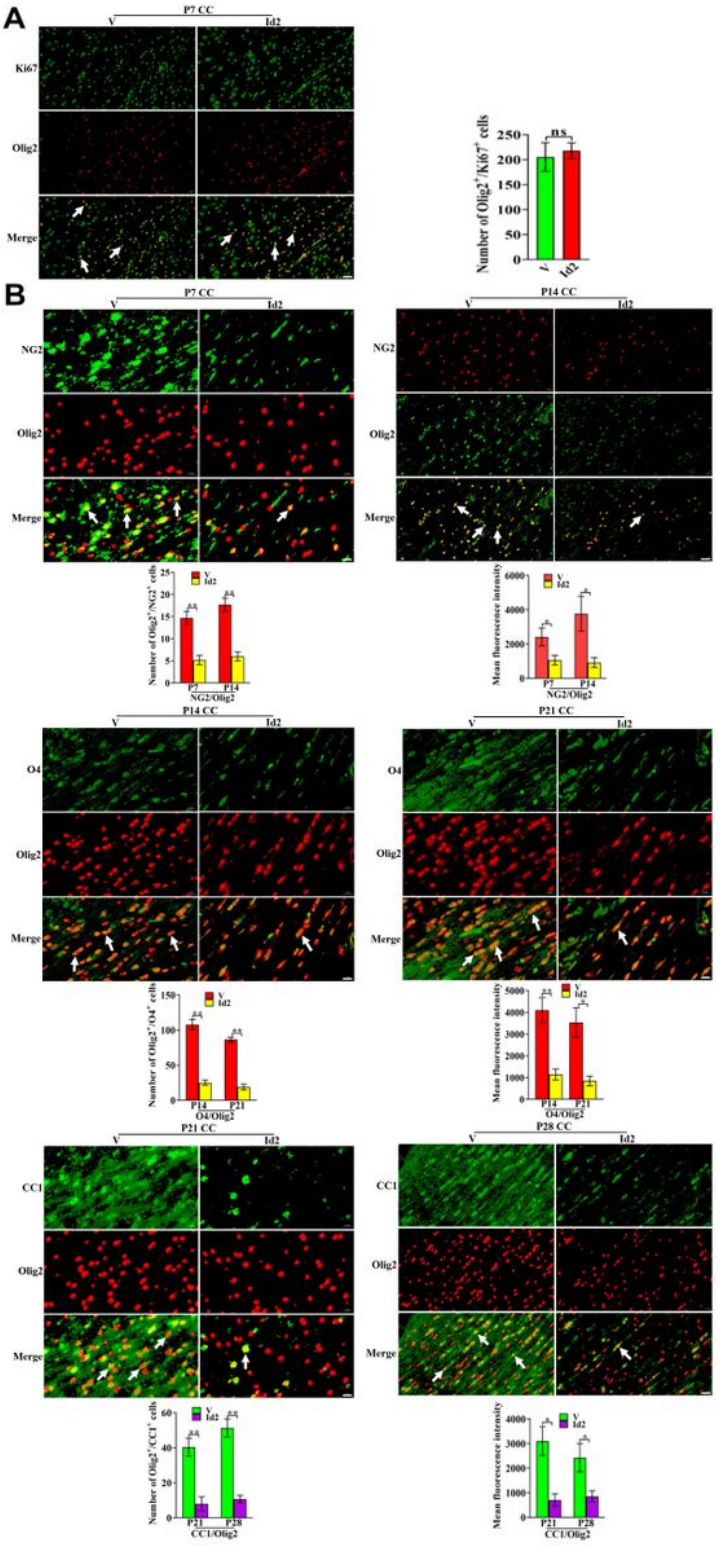

Figure 8

Overexpression of Id2 inhibited OPC differentiation (A) Overexpression of Id2 did not affect OPC proliferation Representative immunofluorescence staining images of Ki67(green) expression via double staining with Olig2(red) at P7. Arrows indicate the Ki67/Olig2 (yellow) positive cells. The number of Ki67/Olig2 positive cells was quantified. It showed that the number of Ki67/Olig2 positive cells was not significantly different in the V and Id2 groups. Scale bar, 20 μm. (B) Overexpression of Id2 hindered the

differentiation of OPC to OL. Representative immunofluorescence staining images of NG2, O4, CC1 (green) expression via double staining with Olig2 (red). Arrows indicate the NG2/Olig2, O4/Olig2, CC1/Olig2 (yellow) positive cells. The number of positive cells and the mean fluorescence intensity were quantified. It showed that the number of NG2/Olig2, O4/Olig2, CC1/Olig2 positive cells and the mean NG2/Olig2, O4/Olig2, CC1/Olig2 fluorescence intensity were significantly decreased in the Id2 group compared with the V group. Scale bar, 20 μm.

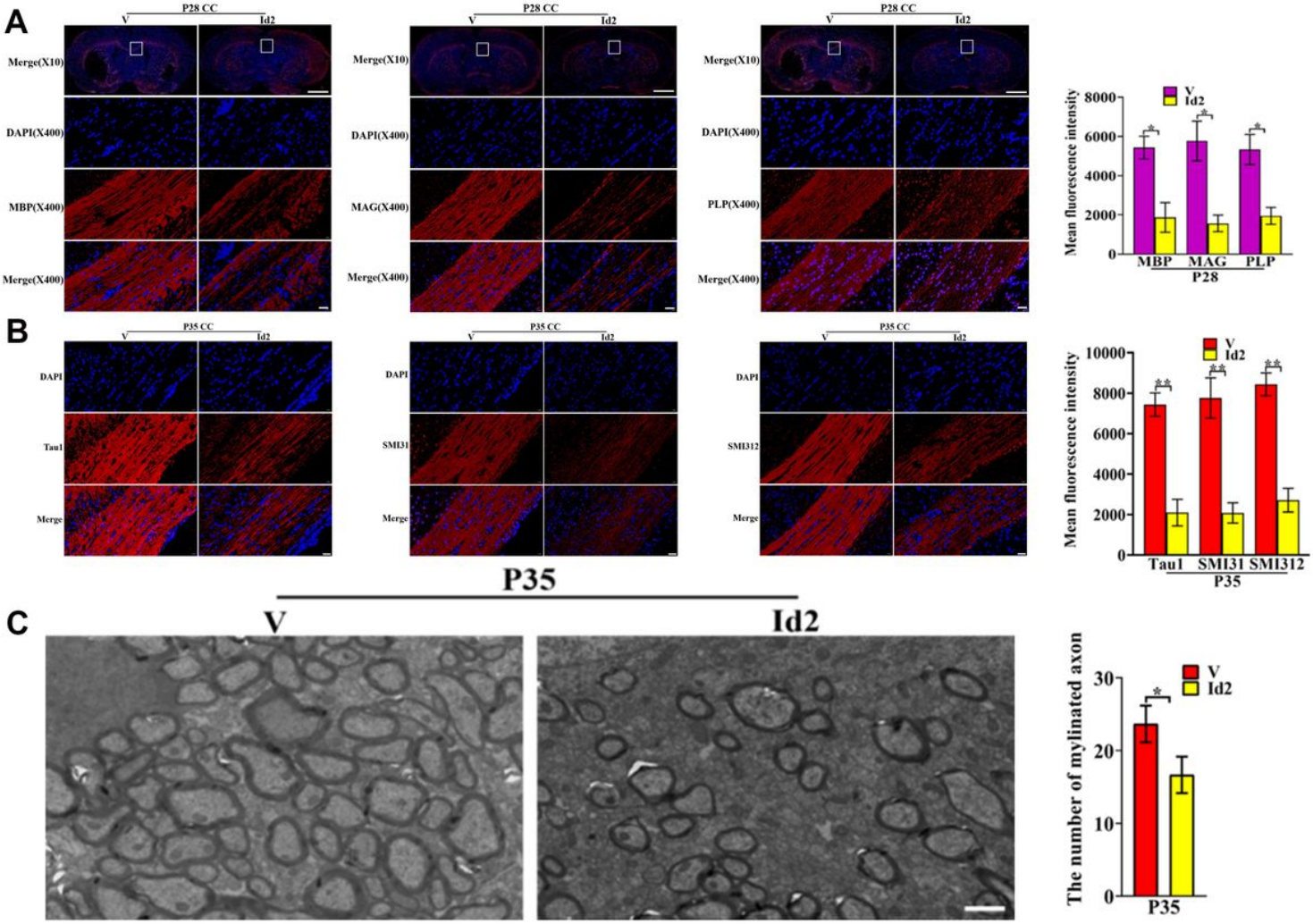

Figure 9

Overexpression of Id2 reversed the effect of Act A on myelination and axon formation (A) Overexpression of Id2 attenuated myelination Representative immunofluorescence staining images of the expression of myelin sheath markers MBP, PLP, and MAG (red) at P28. The mean fluorescence intensity for MBP, PLP, and MAG was quantified. Western blotting and corresponding quantification were performed to measure the expression of MBP, PLP, and MAG. It showed that the expression of MBP, PLP, and MAG was significantly attenuated in the Id2 group compared with the V group. Scale bar, 1000 μm, 20 μm. (B) Overexpression of Id2 attenuated axon formation Representative immunofluorescence staining images of the expression of axon markers Tau1, SMI31, and SMI312(red) at P35. The mean fluorescence intensity for Tau1, SMI31, and SMI312 was quantified. Western blotting and corresponding quantification were

performed to measure the expression of Tau1, SMI31, and SMI312. It showed that the expression of Tau1, SMI31, and SMI312 was significantly attenuated in the Id2 group compared with the V group. Scale bar, 1000 μm, 20 μm. (C) Overexpression of Id2 attenuated myelinated axon formation Representative EM images at P35. It showed that the Id2 group with less myelinated axons compared with the V group. Scale bar, 2 μm.

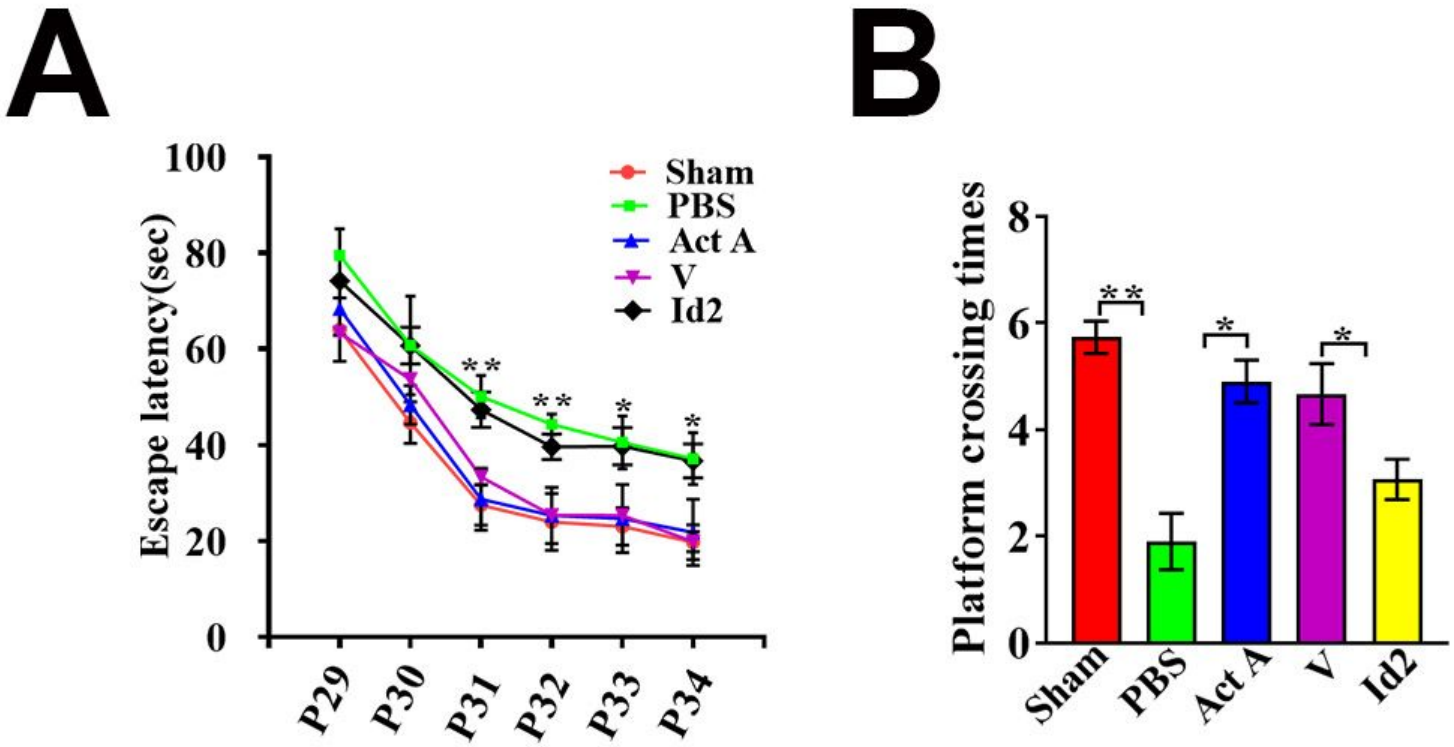

Figure 10

Overexpression of Id2 compromised the behavioral performance of rats after Act A treatment (A) Daily average escape latency of SD rats during the training period It showed that the average escape latency was significantly increased in the Id2 group compared with the V group. (B) The average platform crossing times of SD rats during the test period It showed that the frequency of platform crossing was significantly decreased in the Id2 group compared with the V group.